CrossMark

RESEARCH PAPER

In situ, accurate, surface-enhanced Raman scattering detection of cancer cell nucleus with synchronous location by an alkyne-labeled biomolecular probe

Jing Zhang[1] · Lijia Liang[1] · Xin Guan[2] · Rong Deng[1] · Huixin Qu[2] · Dianshuai Huang[2] · Shuping Xu[1] · Chongyang Liang[2] · Weiqing Xu[1]

Abstract A surface-enhanced Raman scattering (SERS) method for in situ detection and analysis of the intranuclear biomolecular information of a cell has been developed based on a small, biocompatible, nuclear-targeting alkyne-tagged deoxyribonucleic acid (DNA) probe (5-ethynyl-2′-deoxyuridine, EDU) that can specially accumulate in the cell nucleus during DNA replications to precisely locate the nuclear region without disturbance in cell biological activities and functions. Since the specific alkyne group shows a Raman peak in the Raman-silent region of cells, it is an interior label to visualize the nuclear location synchronously in real time when measuring the SERS spectra of a cell. Because no fluorescent-labeled dyes were used for locating cell nuclei, this method is simple, nondestructive, non- photobleaching, and valuable for the in situ exploration of vital physiological processes with DNA participation in cell organelles.

Jing Zhang and Lijia Liang contributed equally to this work.

✉ Shuping Xu
xusp@jlu.edu.cn

✉ Chongyang Liang
liang@jlu.edu.cn

1 State Key Laboratory of Supramolecular Structure and Materials, Institute of Theoretical Chemistry, Jilin University, Changchun, Jilin 130012, China

2 Institute of Frontier Medical Science, Jilin University, Changchun, Jilin 130021, China

Introduction

Understanding the biomolecular dynamics of cancer cells, especially the role of nucleus in the canceration process, is critical for early diagnosis, drug-targeted delivery, and high efficiency therapy. Nucleus as a command center of a cell contains most genetic information of the whole cell and controls cell metabolism and genetic expression. So, for clinical purpose, many anticancer drugs, chemotherapy, and radiotherapy methods were designed for cell nucleus targeting [1–3]. Up to now, more and more nanodrugs have been developed to target cell nucleus rather than just realizing cancer cell delivery with the aim of improving therapeutic efficiency [4, 5]. Meanwhile, analyzing intranuclear biomolecules is also of great significance for expounding molecular mechanisms during external stimuli, especially cancer treatment processes. However, obtaining the molecular information of a cell nucleus with no or little interference in nuclear biological activities still remains a challenge.

Until now, surface-enhanced Raman scattering (SERS) spectroscopy, as one of in situ, nondestructive, fingerprint, and highly sensitive detection methods, has been employed to study the intrinsic information of living cells, organisms, and even in vivo [6–8]. SERS is a plasmon-based technique that requires the probed molecules are adjacent to the plasmonic matters (e.g., gold or silver nanoparticles) that provide greatly amplified local electric field. Thus, plasmon-based nanoprobes with cellular targeting function, low biotoxicity, and SERS ability are needed, which are incubated with cells in

Springer

advance to guarantee that these nanoprobes can accurately access to targeted cells or organelles. Also, their positions in cells are the prerequisite for SERS measurements of intracellular information and they are usually characterized by various microscopies. The commonly used techniques are based on fluorescent imaging and dark-field imaging to pre-confirm the regions of cell nucleus (or cytoplasm) and nanoprobes [9], in which the dye-stained cell organisms become visible in fluorescence imaging and the targeting plasmonic probes are also highlighted in the dark-field imaging (Fig. 1a1). Another option is to label nanoprobes with dyes to make them traceable (Fig. 1a2). Since biosamples show very low contrast grades under the bright-field imaging, it makes quite difficult to locate cell organelles and subcellular regions when SERS detection, the development of the bright/dark-field imaging technique (Fig. 1b), can monitor the location of nanoprobes during the SERS detection process. Based on these locating methods, SERS analysis on many biomolecular events in cancer cells was realized, such as cell mitosis [10] and apoptosis [11] and therapy processes caused by drugs [12] and photothermal treatment [13]. However, there also have been some challenges in precise molecular information detection of subcellular structures using such detection systems: (1) fluorescent labels that are used for staining organelles to highlight their positions may strongly interfere SERS detection or result analysis by producing a broad background or even totally covering most Raman signals, (2) relative bulky structures of florescence dyes also may perturb the activities and functions of living cells, and (3) organelle nanoprobes modified with the targeting ligands cannot be totally accumulated on the regions we are interested in. Therefore, proposing a universal and applicable method for accurate Raman detection of intracellular microregions is still in urgent demand.

Alkyne as a typical molecular marker is often used for biological orthogonal experiments [16, 17]. As we expect, this group is small enough and has very little disturbance to the physiological activities of cells. Especially, its characteristic Raman peak is located in Raman-silent region of cells (1800 −2800 cm^{-1}) [16, 18]. These features illuminate people on the designs of molecular probes with alkyne for Raman bioassays and bioimaging techniques [19, 20], for example, several alkyne-based SERS tags, which can effectively avoid strong organic interferences from resonance-enhanced Raman scattering or autofluorescence since the main bands located at the 2100–2300 cm^{-1} were developed by Hu's group. This work provides an effective solution for multicolor SERS imaging and multiplex sensing when the hyperspectral and intense optical noises are originating from lower wavenumber region. Besides, among alkyne-tagged biomolecules, alkyne-tagged deoxyuridine (5-ethynyl-2′-deoxyuridine, EDU) as a novel

probe has been commonly used for studying cell proliferation since it can competitively infiltrate the deoxyribonucleic acid (DNA) chain as a single base during cell replication, to achieve the purpose of labeling nuclei [21].

Herein, to in situ obtain the precise intranuclear molecular information by SERS, we develop a universal strategy that adopts EDU as an interior label to accurately locate nuclear region without fluorescent dye labeling. The biggest advantage of this method is that we can realize the SERS detection of cell nucleus by a normal Raman spectrometer with no assistance of dark-field or florescence imaging systems. In this design, EDU was first introduced into breast cancer cells (MCF-7) by 24 h co-culturing to ensure enough EDU molecules to specially participate in the DNA replication process, as shown in Fig. 2. Thus, the nuclei of the proliferating cells would be incorporated with EDU. Then, a plasmon-based nuclear-targeting nanoprobe with SERS activity is employed to incubate with cells (Fig. 1c), which can improve Raman sensitivity of both alkynes and cell nucleus during SERS detection. When measuring the SERS spectra of a single cell, EDU's signal existed in the silent spectral range works for an interior label guides us to precisely locate the region of cell nucleus. Therefore, we can convince the obtained SERS spectra are exactly from cell nucleus. This direct SERS study is different from previous reports in which they used alkyne as SERS labeling or SERS probe for indirect SERS determinations [19, 20]. To further evidence the EDU's location in cell, confocal fluorescence microscope was adopted to co-locate EDU (according to a click reaction between alkyne and azide) and nuclei (stained with nuclear-targeting dyes). Our results indicate that the nanoprobe locating and in situ accurate SERS detection of cell nucleus can be synchronously completed. Spectral information pointing to the components of cell nuclei can be selectively analyzed.

Materials and methods

Materials and instrumentation

Ascorbic acid (AA) and silver nitrate (AgNO$_3$) were all of analytical grade and purchased from Beijing Chemical Industry Group Co., Ltd. (Beijing, China). Chloroauric acid (HAuCl$_4$·3H$_2$O, 99.9%), sodium borohydride (NaBH$_4$), cetyltrimethyl ammonium bromide (CTAB), and EDU were obtained from Aladdin. Polyethylene glycol polymer (mPEG-SH, MW = 5000) was obtained from Sigma. Nuclear localization peptide (NLS) (GGVKRKKKPGGC) and NLS-FITC were synthesized by GL Biochem Ltd. (Shanghai, China). Click-iT EdU imaging kit used for confocal fluorescence imaging was obtained from Guangzhou RiboBio Co., Ltd. A JEM-2100F field emission transmission electron microscope (TEM, JEOL, Tokyo, Japan), a confocal Raman spectrometer
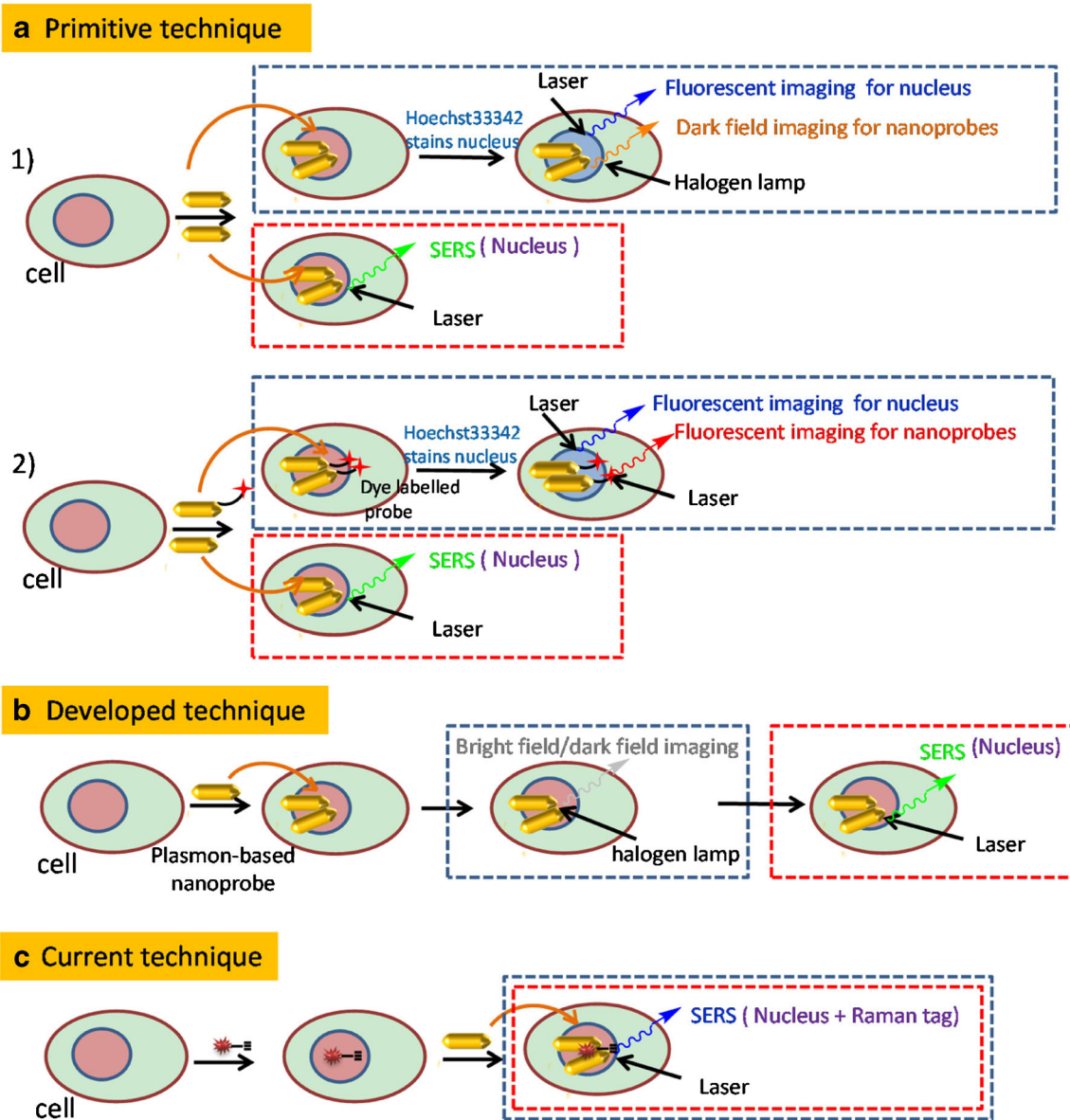
Fig. 1 Progress of cell nucleus locating (blue frame) and SERS detection (red frame). **a** Primitive technique: pre co-location of dark-field imaging (for nanoprobe) and fluorescent imaging (for nucleus) before measuring SERS spectra of nucleus [14, 15]. **b** Developed technique: finding nanoprobes by bright-field/dark-field imaging and SERS detection of nucleus [11]. **c** Current technique: implanting interior label (EDU) in nucleus and measuring SERS of nucleus simultaneously

(LabRAM Aramis, Horiba Jobin Yvon) with the 633-nm excitation laser (He–Ne laser, UNIPHASE), an ultraviolet–visible spectrometer (Ocean Optics, USB4000), a dynamic light scattering (DLS, Malvern Zetasizer Nano ZS) system, a laser scanning confocal microscope (Olympus FV1000), a microplate reader (Austria GmbH, 16039400), a Delta Vision OMX Imaging System with 3D SIM model from GE Healthcare (No. OM06051, Pittsburgh, PA, USA), Imaris X 64 from Bitplane (Zurich, Switzerland) analysis software, and a self-built dark-field/fluorescence microscope (Olympus, with a ×20/0.4 N.A. objective, more details are provided in reference [8], were used in our experiment.

Cell culture, EDU, and AuNR incubation

Breast cancer cells (MCF-7), purchased from Shanghai ATCC cell bank, were cultured in Dulbecco's modified Eagle's medium (DMEM, Gibco) supplemented with 10% (v/v^{-1}) fetal bovine serum (FBS, Mediatech) and 1% of antimycotic solution (Mediatech) at 37 °C in a humidified atmosphere containing 5% CO_2 incubator. Cells were collected at logarithmic growth stages by centrifugation at 1000 rpm for 5 min and then were cultured on coverslips. One hundred microliters of EDU was added to 1.9 mL of cell culture solution for 24 h. Then, these MCF-7 cells were further incubated with the

Fig. 2 Schematic illustration of the SERS detection of cancer cell nucleus with EDU as an interior label and the AuNR-based nuclear-targeting probe
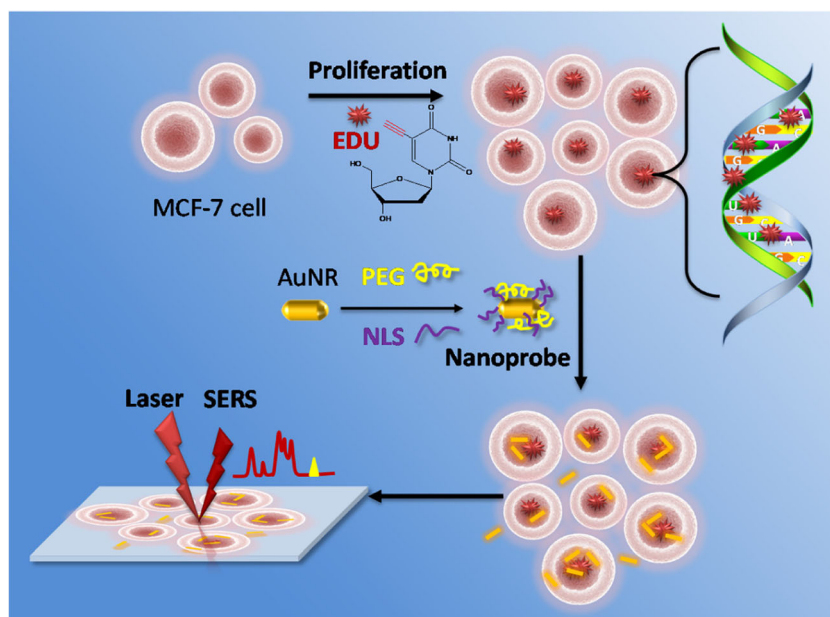
nuclear-targeting nanoprobes (AuNRs-PEG-NLS, 0.05 nM) for 12 h and fresh cell culture medium in each well. The synthesis and modification of AuNRs and more experimental details can be found in the Electronic Supplementary Material (ESM). After incubation, the coverslips were washed three times with PBS to remove excess nanoprobes, and then, the cells were fixed with 4% formaldehyde for 20 min.

Cell viability assay

Cell viability was measured by the WST-1 (2-(4-iodophenyl)-3-(4-nitrophenyl)-5-(2,4-disulfophenyl)-2H-, tetrazolium monosodium salt) assay. MCF-7 cancer cells were firstly seeded in a 96-well plate for 24 h with EDU and then treated with 0.05 nM nanoprobes. After 12-h incubation, 10 μL of the WST-1 solution was added into each well and the plant was incubated for 1 h. Finally, the 96-well plate was measured with a microplate reader instrument with the excitation of 450 nm for fluorescence intensity measurements.

Location of EDU in nucleus by fluorescence microscopes

Cells were cultured with 200 μM of EDU for 24 h in the culture plate. After incubation, the coverslips were cleaned two times with PBS, each time for 5 min, fixed with 4% formaldehyde for 30 min at room temperature, and further cleaned with PBS. Permeabilization buffer (0.5% Triton X-100 PBS) was added in each wells and kept in a shaker for 10 min twice. Then, cells were incubated with an Apollo® staining solution (Apollo® 643-azide, Click-iT Imaging Kit) for 30 min at room temperature in dark to stain EDU according to a click reaction between alkyne and azide. And then, the permeabilization buffer was added in above cell well to

increase the permeability of cell membrane. Cells were then washed with methanol and PBS. Finally, they were incubated with Hoechst 33342 (10 μg mL^{-1}) for 30 min at room temperature in dark. After removing nuclear dye with PBS washing three times, the images were observed under a laser scanning confocal microscope (Olympus FV1000).

## Location of nanoprobes in nuclei by dark-field/fluorescence imaging

The cells grown on a slide glass for 24 h were incubated with the nuclear-targeting SERS-active nanorods for 12 h and next stained by Hoechst 33342 (10 μg mL^{-1}). Cells were transferred to a cover glass for dark-field imaging by a self-built microspectroscopic system with a ×20/0.40 N.A. objective. To take the images of the Hoechst 33342-stained nuclei, a mercury lamp was used and a filter cube with the excitation wavelength of 390–435 nm and emission of 488 nm was fixed in the light path.

Intranuclear distribution of nanoprobes by high-resolution 3D confocal fluorescence microscope

To take the fluorescent images of the nuclear-targeting nanoprobes inside cells, the FITC-labeled AuNRs-PEG-NLS were also needed. After cells were cultured with 0.05 nM of the FITC-labeled AuNRs-PEG-NLS for 12 h, the individual cell fluorescent images were taken by a DeltaVision OMX Imaging System with 3D SIM model from GE Healthcare (No. OM06051, Pittsburgh, PA, USA). An analysis software, Imaris X 64 from Bitplane (Zurich, Switzerland), was further used to deal with image data and build 3D views.

Fig. 3 a TEM image of AuNRs. **b** UV–vis spectra of the AuNRs (black), AuNRs-PEG (blue), and AuNRs-PEG-NLS (red). **c** Zeta potential of AuNRs before and after modified with PEG and NLS. **d** Cell viability of MCF-7 cells incubated with EDU, AuNRs-PEG-NLS, and AuNRs-PEG-NLS and EDU, respectively. The concentrations of nanoprobes and EDU are 0.05 nM and 200 μM. **$p < 0.005$ analyzed by t test
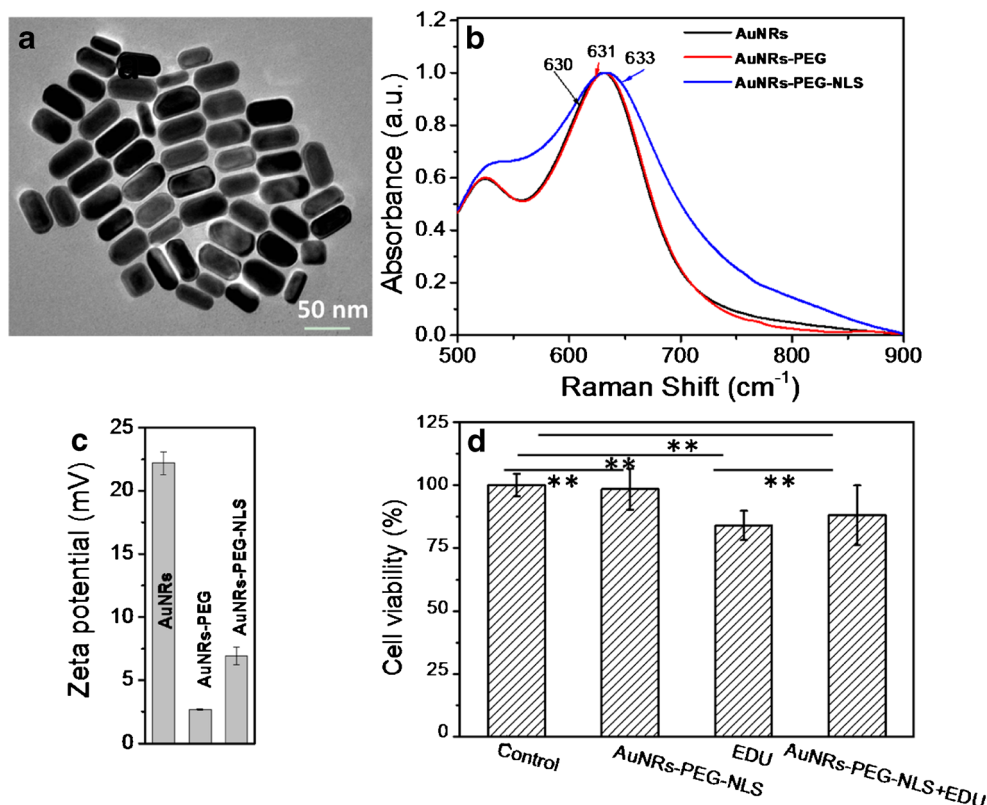
Results and discussion

In order to obtain molecular information of cell nucleus by SERS spectroscopy, a plasmon-based nuclear-targeting nanoprobe is required, since the Raman spectra of cell nucleus are much weak and no obvious signals can be observed (see ESM Fig. S1). Here, we adopted the nuclear-targeting nanoprobe based on AuNR due to its controllable size and localized surface plasmon resonance (LSPR) features, easy surface modification, strong light scattering, and excellent SERS enhancement activity. The preparation of this nuclear-targeting nanoprobe is based on our previous report [14, 15]. AuNRs with an average aspect ratio of 2.3 (62 nm × 27 nm, Fig. 3a) and the longitudinal plasmon mode at 632 nm were synthesized and used in the present study. Next, a thiol-modified polyethylene glycol (PEG-SH, 5000) and a NLS (GGVKRKKKPGGC) [22] were attached to the surfaces of AuNRs, since the PEG can avoid absorbing nonspecific proteins in culture medium and the NLS can effectively help the AuNR transfer to the nuclei through combining a nuclear transport protein importin [23] which can accelerate the passing action through the nuclear pore complexes [24, 25]. After surface modification, the plasmonic features of AuNRs-PEG and AuNRs-PEG-NLS have almost no obvious changes compared with AuNRs (Fig. 3b), while the zeta potentials of AuNRs show noticeable changes from 22 to 2.7 and 6.9 mV (Fig. 3c) when the positively charged surfactant (hexadecylcetyltrimethyl ammonium bromide, CTAB) were replaced by PEG and NLS. Moreover, the obtained AuNRs-PEG-NLS probe was evaluated by the WST-1 assay, which shows the cell viability is above 98% after cells have been incubated with 0.05 nM of nanoprobes for 24 h (marked as AuNRs-PEG-NLS in Fig. 3d).

To evaluate the nuclear-targeting ability of our designed nanoprobe, we used the dark-field and fluorescence co-locating to investigate the distributions of AuNRs-PEG-NLS (Fig. 4a, b). From the dark-field/fluorescent merged image (Fig. 4), we can find that AuNRs can be delivered to cell nuclei with the help of NLS (Fig. 4b) compared with AuNRs-PEG (Fig. 4a). While owing to the cell that is a 3D structure, we used the high-resolution 3D fluorescence imaging to further precisely locate the distributions of these nanoprobes. Here, we decorated the nanoprobes with the fluorescent dye (FITC)-labeled NLS instead of the NLS to trace the positions of nanoprobes by the fluorescence of FITC. Based on the high-resolution 3D views of the FITC and Hoechst 33342 (Fig. 4c, A–D), we found that although most AuNRs-PEG-NLS nanoprobes have been successfully delivered to cell nuclei, many of them are still outside the cell nucleus region or in the cytoplasm. The reasons for the failure nuclear-targeting delivery of some nanoprobes can be explained from the failed binding between NLS and nuclear transport protein importin and some oversized AuNRs, which causes AuNRs remaining in cytoplasm. So, if we collect SERS spectra of cells with the guidance of nuclear-targeting nanoprobes only, some spectra that are not originated

Fig. 4 The dark-field, dark-field/ fluorescent merged, and bright-field images of the intranuclear distributions of the AuNRs-PEG (**a**) and AuNRs-PEG-NLS nanoprobes (**b**), taken by a self-built dark field/fluorescence imaging microscope. MCF-7 cells were treated with 0.05 nM of nanoprobes (AuNRs-PEG-NLS) for 12 h and then the nucleus with Hoechst 33342 stained. The blue color represents nuclei, while the yellow scattering is from AuNRs. (**c**) The confocal fluorescent image (A) of the intranuclear distributions of the FITC-labeled nanoprobes and the high-resolution 3D view images (B, C, and D) of the individual cell. The blue color represents the nucleus of cancer cell stained with Hoechst 33342, while the green indicates the FITC-labeled AuNRs-PEG-NLS. This image is detected by a DeltaVision OMX Imaging System with 3D SIM model from GE Healthcare (No. OM06051, Pittsburgh, PA, USA) and analyzed via Imaris X 64 software from Bitplane (Zurich, Switzerland). B is the panorama of the cell and C is the magnified area of marked position in B. D is the perspective of FITC-labeled nanoprobes within the nuclei
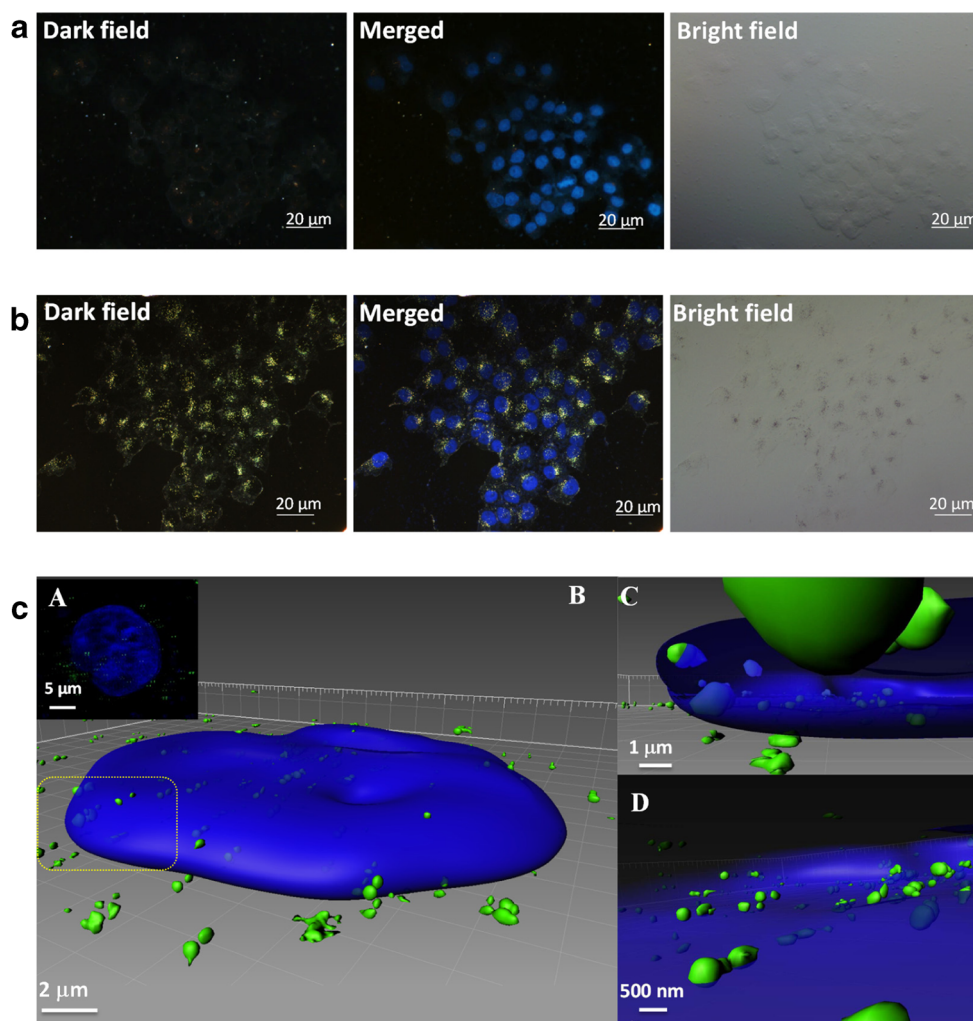
from cell nucleus will also be obtained, which advances us to get the accurate SERS spectra of cell nucleus with the additional labeling.

To determine accurate cell nucleus region and obtain the molecular information, we selected the EDU molecule to locate the position of cell nucleus since it can incorporate with DNA chains in nucleus. First, we employed the confocal fluorescence microscope to co-locate Hoechst 33342-stained nuclei and EDU according to a click reaction between alkyne and azide. As shown in Fig. 5, when MCF-7 cells were incubated with 200 μM of EDU for 24 h in a culture plate and were then stained through the Click-iT Imaging Kit, their cell nuclei show red color under 635 nm excitation, while the nuclei were stained by Hoechst 33342, showing blue under the excitation light of 405 nm. The merged image shows two colors overlapped in most nuclei, confirming that EDU molecules can identify cell nuclei. The high-magnification images of single cell shown in the top panel can clearly indicate that EDU can target cell nucleus. To assess the nuclear-targeting ability of EDU, several florescence images of cell nuclei stained with Hoechst 33342 and EDU were analyzed by ImageJ software.

The nuclear labeling efficiency can reach 95.1 ± 1.9%, which demonstrates EDU processes the high nucleus labeling ability. To estimate the effects of EDU on physiological activities and nuclear functions, the cell viability test of MCF-7 treated with 200 μM of EDU for 24 h was performed (marked as EDU in Fig. 3d). The cell viability result illustrates that such an amount of EDU has little damage to MCF-7 cells.

To further confirm whether the EDU can be treated as an interior signal label in the SERS detection of cell nucleus, we recorded the spontaneous Raman and SERS spectra of EDU molecule without or with nuclear-targeting nanoprobes, respectively. As shown in Fig. 6a, we can find the featured peaks of EDU at 780, 1235, 1617, 1669, and 2118 cm^{-1}. Among them, the noticeable peak at 2118 cm^{-1} in Raman spectrum is assigned to the C≡C vibration mode, while the SERS spectrum of EDU displays obvious differences. One of notable changes is that the C≡C vibration mode of EDU divides into two peaks, located at 1999 and 2058 cm^{-1}, which is consistent with previous studies that the C≡C peak changed obviously when it interacted with a silver SERS substrate [26–28]. For the obvious Raman shift, it is possible that there is a strong
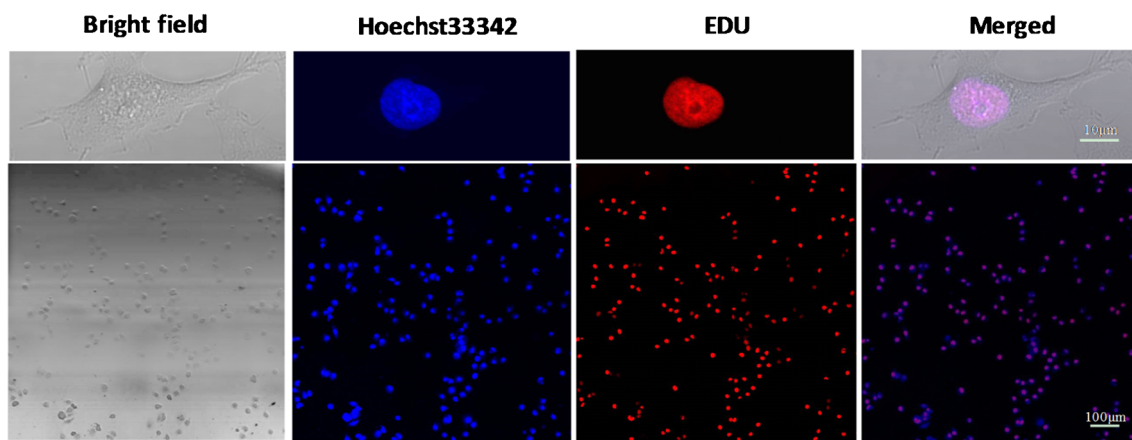
Fig. 5 Confocal fluorescent images of MCF-7 cells cultured with 200 μM of EDU. The cell nuclei were stained with Hoechst 33342 to display blue (excitation by 405 nm light) and EDU were highlighted by red due to a click reaction between alkyne and azide (excitation by 635 nm light). The top panel displays the enlarged images of individual MCF-7 cell

interaction between EDU and the SERS substrate. Another is that intensity of the two peaks is low compared with the C≡C peak in Raman spectrum as shown in Fig. 6(I). SERS intensity may be affected by many factors, for example, the local electromagnetic field, the chemical interaction, and the concentrations of the analyst. Even the surrounding medium also can affect the SERS intensity. While even the peak relative intensities decrease remarkably and the C≡C peaks shift obviously, these two peaks are traceable since they are in the Raman-silent region of cells.

To obtain the SERS spectra of cell nucleus with the assistance of EDU precise nuclear location ability and SERS enhancement from nuclear-targeting nanoprobe, MCF-7 cells treated with EDU in the proliferation process followed with AuNRs-PEG-NLS nanoprobes for 12-h incubation. In this condition, the cell viability of MCF-7 is 88 ± 11% (marked as AuNRs-PEG-NLS+EDU in Fig. 3d), ensuring our method has low damage toward cells. As shown in Fig. 6b, we can observe that two obvious peaks at 1920 and 2265 cm^{-1} of SERS spectrum obtained from MCF-7

cells treated with EDU and nuclear-targeting nanoprobe. Owing to peaks at 1920 and 2265 cm^{-1} in the Raman-silent region of cells are much different with the SERS signals from alkyne group of EDU solution (1999 and 2058 cm^{-1}), it is necessary to make sure whether the peaks (1920 and 2265 cm^{-1}) are produced by the alkyne group. So, the SERS spectra of MCF-7 without EDU from different locations were also collected. No obvious peaks can be found in the Raman-silent region of cells, confirming that the signals at 1920 and 2265 cm^{-1} are indeed derived from EDU. The reason why the SERS signal of alkyne group in solution show noticeable difference from that in cell is still needed to be further explored [26–28]. Also, we can conclude that both EDU molecule and nuclear-targeting nanoprobe are needed to obtain the SERS spectra of cell nucleus since the spontaneous Raman spectrum is relative weak compared with SERS spectrum (shown in Fig. 6b).

Figure 7c (also in ESM Fig. S2) shows the SERS spectra of one cell from different positions marked as Fig. 7a. SERS spectra from A to E show the obvious peaks at 1920 and
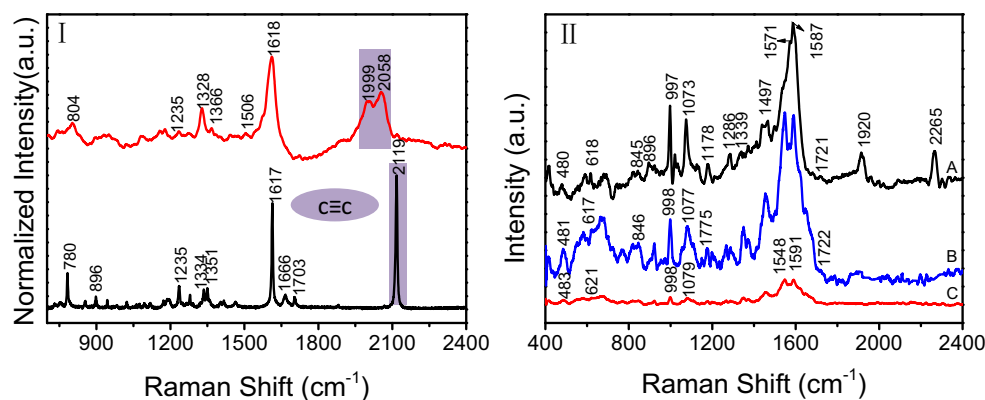
Fig. 6 (I) Spontaneous Raman (bottom) and SERS spectra (top) of 2 μM of EDU, with the laser power of 7.1 mW, a collection time of 20 s, and two accumulations. (II) Spontaneous Raman (C) and SERS spectra (A and B) of nucleus of MCF-7 cells without and with AuNRs-PEG-NLS (0.05 nM). SERS spectra (A) of nucleus of MCF-7 cells with 200 μM EDU, with the laser power of 4.3 mW, a collection time of 40 s, and two accumulations
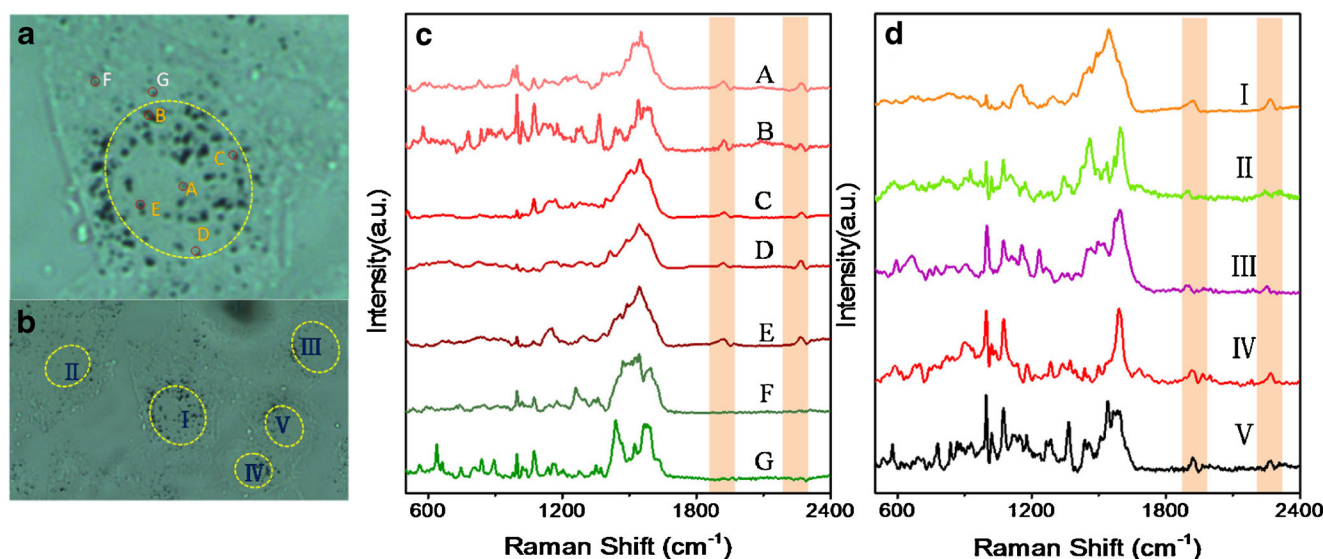
Fig. 7 Bright-field image of one (a) and five cancer cells (b) treated with nucleus targeting nanoprobes (0.05 nM). (c) SERS spectra of the cell obtained from the spots marked as A–G in (a). (d) SERS spectra of nuclei collected from different cells as (b). All spectra were obtained by a Raman spectrometer (LabRAM ARAMIS, HORIBA JobinYvon) equipped with a 633-nm laser, with the laser power of 4.3 mW, a collection time of 40 s, and two accumulations

Table 1 The assignments of the SERS bands collected from the nuclei of MCF-7 cells

Raman shift (cm^{-1})	DNA	Assignments of protein/lipid
506		S-S
577/1360/1553		Trp
663		ν(C-S)
741		C-S
780/837	O-P-O	
840/1177		Tyr
904/944/1145/1448	Dr-P	
980	Dr	
997		Phe
1021/1039	Dr ν(C-O)	
1072	Dr ν(C-O)	C-N ν(C-O),ν(C-O-C)
1238	U,C	
1261/1286	T	AmideIII
1365/1438		γ(CH$_2$/CH$_3$)
1386		γ(CH$_3$)
1485/1492/1570	G,A	
1505/1519	A	
1534/1540	A,C,G	
1580	G,A	
1585		-N$_7$-H$_7$
1621	U	

A adenine, *C* guanine, *U* uracil, *T* thymine, ν stretch, γ bending vibration, *Dr-P* deoxyribose-phosphoric acid, *phe* phenylalanine, *Tyr* tyrosine, *Trp* tryptophan

2265 cm^{-1} in the Raman-silent region of cells, while the SERS spectra of F and G almost presented no obvious peaks in the same spectral range. Thus, SERS spectra of A–E presenting SERS signals at 1920 and 2265 cm^{-1} are from the nuclear region, which means we can obtain the precise SERS spectra of intranuclear information. Figure 7d shows the intranuclear information of different cells marked in Fig. 7b, proving our method is universally valid for nuclear SERS targeting detection.

Using this method, we obtained the precise SERS spectra from cell nucleus region. Then, we assigned and analyzed the intranuclear molecular information. Assignments of the peaks are listed in Table 1. From Fig. 7c (curves of A–E), the main peaks are located at 900–1500 cm^{-1}. Among them, 1261 cm^{-1} (T), 1286 cm^{-1} (T), 1485 cm^{-1} (G, A), 1492 cm^{-1} (G, A), 1505 cm^{-1} (A), 1519 cm^{-1} (A), 1534 cm^{-1} (A, C, G), 1570 cm^{-1} (G, A), and 1580 cm^{-1} (G, A) originated from DNA bases. The peaks of 1238 cm^{-1} (U, C) and 1621 cm^{-1} (U) come from the EDU probe, which we can find these two peaks from EDU in solution (Fig. 6). Also, the 1081-cm^{-1} band that contributed to the symmetric extension of O=P=O is observed. As we know, cell nucleus not only includes abundant genetic information but also various proteins. So, the peaks of 577 cm^{-1} (Trp), 997 cm^{-1} (Phe), 1072 cm^{-1} (C-N), and 1286 cm^{-1} (AmideIII) all come from the vibrational information of proteins.

Considering the differences of functions and molecular composition between nucleus and cytoplasm, we probed their molecular information by our proposed strategy. By comparing with the SERS spectra of nucleus, cytoplasm gives rich spectral information in the range of 600–1600-cm^{-1} (F and G)

Table 2 Comparison of SERS spectra between nucleus and cytoplasm in MCF-7 cells

Assignments for nucleus	Raman shift (cm^{-1})	Assignments for cytoplasm	Raman shift (cm^{-1})
S-S	506	S-S	501
Tyr	840/1177	ν(C-S)	663
Dr	980	C-S	741
Phe	997	Tyr	840
ν(C-N)	1072	ν(C-C)	895
AmideIII	1261	Phe	997
U,C	1238	Phe	1039
Trp	1360	ν(C-N)	1072
γ(CH$_2$/CH$_3$)	1438	Tyr/Phe	1204
Dr-P	1448	AmideIII	1261
G,A	1485	Trp	1351
A	1519	Trp	1360
A,C,G	1534	Gluc	1373
Trp	577/1360/1553	γ(CH$_2$/CH$_3$)	1438
G,A	1485/1492/1570	AmideII	1560
A,G	1580	Phe	1621
U	1621		

Raman bands associated with proteins and lipids are noticeable in SERS spectra from cytoplasm. The peaks assigned to protein are observed at 840 cm^{-1} (Tyr), 997 cm^{-1} (Phe), 1039 cm^{-1} (Phe), 1204 cm^{-1} (Tyr, Phe), 1351 cm^{-1} (Trp), and 1621 cm^{-1} (Phe), while lipid backbone bands at 1072 cm^{-1} (C–O, C-O-C symmetric stretching) and 1371 cm^{-1} (CH$_2$ wagging) are also found. Obvious differences of these spectra can also be found in Table 2. Furthermore, SERS spectra of different positions from the same nucleus or cytoplasm were not completely identical, which can be explained by the complexity of the intracellular compositions. The above results confirm that EDU as a nucleus localization interior label can allow us to realize accurate location of nuclei, and with its assistance, we can investigate the biomolecules from the cell nucleus by SERS.

Conclusion

With the aim of in situ obtaining precise SERS spectra of nucleus and analyzing its biomolecular information, we proposed a method that EDU as an interior label by competitive infiltrating on the replicated DNA molecules, to accurately locate cell nuclei. With the plasmon-based nuclear-targeting nanoprobe as SERS substrate, we explored molecular information of cancer cell nucleus by in situ SERS spectroscopy with high sensitivity and accuracy. Our strategy can realize the detection locating and the SERS measurement synchronously, which is superior to previous studies in which these two procedures are carried out individually. The intrinsic molecular information of cell nucleus was discussed and compared with cytoplasm. This strategy provides the possibility for us to explore and expound the mechanisms of drug and radiation therapy.

Compliance with ethical standards

Conflict of interest The authors declare that they have neither financial nor nonfinancial conflicts of interest.

Ethics Breast cancer cells (MCF-7) belong to cell line and we bought this cell line from Shanghai ATCC cell gank, which granted the permission of the Human Research Ethics Committee of the country for manipulations of human cells.

References

1. Tewey KM, Rowe TC, Yang L, Halligan BD, Liu LF. Adriamycin-induced DNA damage mediated by mammalian DNA topoisomerase II. Science. 1984;226:466–8.
2. Zhou Z, Shen Y, Tang J, Fan M, Van Kirk EA, Murdoch WJ, et al. Charge-reversal drug conjugate for targeted cancer cell nuclear drug delivery. Adv Funct Mater. 2009;19:3580–9.
3. Fan WP, Shen B, Bu WB, Zheng XP, He QJ, Cui ZW, et al. Design of an intelligent sub-50 nm nuclear-targeting nanotheranostic system for imaging guided intranuclear radiosensitization. Chem Sci. 2015;6:1747–53.
4. Pan L, He Q, Liu J, Chen Y, Ma M, Zhang L, et al. Nuclear-targeted drug delivery of TAT peptide-conjugated monodisperse mesoporous silica nanoparticles. J Am Chem Soc. 2012;134:5722–5.

5. Fan W, Shen B, Bu W, Zheng X, He Q, Cui Z, et al. Intranuclear biophotonics by smart design of nuclear-targeting photo-/radio-sensitizers co-loaded upconversion nanoparticles. Biomaterials. 2015;69:89–98.

6. Cheng J, Xie X. Vibrational spectroscopic imaging of living systems: an emerging platform for biology and medicine. Science. 2015;350:aaa8870.

7. Qian X, Peng XH, Ansari DO, Yin-Goen Q, Chen GZ, Shin DM, et al. In vivo tumor targeting and spectroscopic detection with surface-enhanced Raman nanoparticle tags. Nat Biotechnol. 2008;26:83–90.

8. Taketani A, Hariyani R, Ishigaki M, Andriana BB, Sato H. Raman endoscopy for the in situ investigation of advancing colorectal tumors in live model mice. Analyst. 2013;138:4183–90.

9. Li H, Wang H, Huang D, Liang L, Gu Y, Liang C, et al. Note: Raman microspectroscopy integrated with fluorescence and dark field imaging. Rev Sci Instrum. 2014;85:056109.

10. Panikkanvalappil SR, Hira SM, Mahmoud MA, El-Sayed MA. Unraveling the biomolecular snapshots of mitosis in healthy and cancer cells using plasmonically-enhanced Raman spectroscopy. J Am Chem Soc. 2014;136:15961–8.

11. Kang B, Austin LA, El-Sayed MA. Observing real-time molecular event dynamics of apoptosis in living cancer cells using nuclear-targeted plasmonically enhanced Raman nanoprobes. ACS Nano. 2014;8:4883–92.

12. Austin LA, Kang B, El-Sayed MA. A new nanotechnology technique for determining drug efficacy using targeted plasmonically enhanced single cell imaging spectroscopy. J Am Chem Soc. 2013;135:4688–91.

13. Aioub M, El-Sayed MA. A real-time surface enhanced Raman spectroscopy study of plasmonic photothermal cell death using targeted gold nanoparticles. J Am Chem Soc. 2016;138:1258–64.

14. Liang L, Huang D, Wang H, Li H, Xu S, Chang Y, et al. In situ surface-enhanced Raman scattering spectroscopy exploring molecular changes of drug-treated cancer cell nucleus. Anal Chem. 2015;87:2504–10.

15. Deng R, Qu H, Liang L, Zhang J, Zhang B, Huang D, et al. Tracing the therapeutic process of targeted aptamer/drug conjugate on cancer cells by surface-enhanced Raman scattering spectroscopy. Anal Chem. 2017;89:2844–51.

16. Yamakoshi H, Dodo K, Okada M, Ando J, Palonpon A, Fujita K, et al. Imaging of EdU, an alkyne-tagged cell proliferation probe, by Raman microscopy. J Am Chem Soc. 2011;133:6102–5.

17. Wei L, Hu F, Shen Y, Chen Z, Yu Y, Lin CC, et al. Live-cell imaging of alkyne-tagged small biomolecules by stimulated Raman scattering. Nat Methods. 2014;11:410–2.

18. Yamakoshi H, Dodo K, Palonpon A, Ando J, Fujita K, Kawata S, et al. Alkyne-tag Raman imaging for visualization of mobile small molecules in live cells. J Am Chem Soc. 2012;134:20681–9.

19. Lin L, Tian X, Hong S, Dai P, You Q, Wang R, et al. A bioorthogonal Raman reporter strategy for SERS detection of glycans on live cells. Angew Chem Int Ed. 2013;52:7266–71.

20. Chen Y, Ren JQ, Zhang XG, Wu DY, Shen AG, Hu JM. Alkyne-modulated surface-enhanced Raman scattering-palette for optical interference-free and multiplex cellular imaging. Anal Chem. 2016;88:6115–9.

21. Salic A, Mitchison TJ. A chemical method for fast and sensitive detection of DNA synthesis in vivo. PNAS. 2008;105:2415–20.

22. Huefner A, Kuan WL, Barker RA, Mahajan S. Intracellular SERS nanoprobes for distinction of different neuronal cell types. Nano Lett. 2013;13:2463–70.

23. Kang B, Mackey MA, El-Sayed MA. Nuclear targeting of gold nanoparticles in cancer cells induces DNA damage, causing cytokinesis arrest and apoptosis. J Am Chem Soc. 2010;132:1517–9.

24. Pante N, Kann M. Nuclear pore complex is able to transport macromolecules with diameters of similar to 39 nm. Mol Biol Cell. 2002;13:425–34.

25. Tkachenko AG, Xie H, Coleman D, Glomm W, Ryan J, Anderson MF, et al. Multifunctional gold nanoparticle-peptide complexes for nuclear targeting. J Am Chem Soc. 2003;125:4700–1.

26. Joo S-W, Kim K. Adsorption of phenylacetylene on gold nanoparticle surfaces investigated by surface-enhanced Raman scattering. J Raman Spectrosc. 2004;35:549–54.

27. Kennedy DC, McKay CS, Tay LL, Rouleau Y, Pezacki JP. Carbon-bonded silver nanoparticles: alkyne-functionalized ligands for SERS imaging of mammalian cells. Chem Commun. 2011;47:3156–8.

28. Ando J, Asanuma M, Dodo K, Yamakoshi H, Kawata S, Fujita K, et al. Alkyne-tag SERS screening and identification of small-molecule-binding sites in protein. J Am Chem Soc. 2016;138:13901–10.